# Coupling between electrokinetics and electrode kinetics by bipolar faradaic depolarisation processes in microfluidic channels

Jérôme F.L. Duval, Herman van Leeuwen

# Coupling between electrokinetics and electrode kinetics by bipolar faradaic depolarisation processes in microfluidic channels

Jérôme F.L. Duval,[1*] and Herman P. van Leeuwen[2]

[1] CNRS-Université de Lorraine, Laboratoire Interdisciplinaire des Environnements Continentaux (LIEC), UMR 7360 CNRS, 15 avenue du Charmois, F-54500 Vandœuvre-lès-Nancy, France.
[2] Physical Chemistry and Soft Matter, Wageningen University & Research, Stippeneng 4, 6708 WE Wageningen, The Netherlands.

[*]Corresponding author: jerome.duval@univ-lorraine.fr. Tel: 00 33 3 72 74 47 20.

## Abstract

This article is concerned with the nature and impact of bipolar faradaic electron transfer processes in the context of measuring electrokinetic parameters at the interface between an electronically conductive substrate such as a solid metal layer, and a liquid medium. More specifically, it analyses the steady state electric current through the electrodic substrate layer in terms of its short-circuiting effect on the system's electrokinetic quantities, such as the streaming potential. Ample attention is paid to the electrodic behaviour of the chosen metal and its electron transfer characteristics with respect to redox functions in the medium. The electrochemical reversibility of redox couple species is expressed in terms of their oxidation and reduction rate constants as compared to their diffusive transport rates under lateral flow conditions. High values for rate constants lead to high reversibilities and large bipolar leaking currents through the metal substrate. In turn, high electron transfer rate constants generate large reductions in measured values for electrokinetic quantities such as streaming potentials that become a non-linear function of the pressure gradient applied through the fluidic chamber. The present article presents an overview of theoretical and experimental approaches of this intricate coupling between bipolar electrode kinetics and electrokinetics and the impact from Hans Lyklema's contributions. It highlights not only the implications of bipolar faradaic depolarisation processes in electrokinetics but also the importance of bipolar electrochemistry principles in various electroanalytical applications reported for *e.g.* the control of microfluidic flows, for surfaces functionalisation, particles manipulation or for the wireless detection of electroactive analytes.

Keywords: Bipolar electrochemistry, Electrokinetics, Electrode kinetics, Streaming potential, Microfluidics.

This paper is part of the Hans Lyklema tribute issue.

## Contents of paper

## 1. Introduction

Electrokinetic phenomena such as streaming potentials and electrophoresis of dispersed particles have played crucial roles in the development of the physical chemistry of colloids [1,2]. Those who have known Prof. Hans Lyklema (1930-2017) and his team at Wageningen University (The Netherlands) will not be surprised that Hans has often found himself immersed in fundamental electrokinetic research issues, from the very beginning [3] till the end [4] of his career. The few electrodic electrochemists in the group generally had a hard time following the electrokinetic line of thinking since the transversal orientation of electrodic electron transfer processes at the substrate surface does not easily match with the tangential orientation of the external electric field as applied in electrokinetic measurements. Yet there are conditions under which electrokinetic phenomena, as a part of colloid chemistry, are intimately coupled with the electrodic processes occurring in electrochemistry [5].

The measured electrokinetic quantities reflect the double layer properties of the surface/solution interface, in particular the zeta ($\zeta$)-potentials for hard impermeable surfaces [1-6], and the space charge density and hydrodynamic softness for soft surfaces [7-11]. Streaming potential is by far the most widely used experimental quantity to probe double layer properties of flat surfaces [1]. It is the steady state potential difference generated by the flow of liquid along a charged surface in a capillary or a thin-layer cell. The feasibility of the technique for conducting surfaces like metals has been questioned because the strong electronic conduction in the bulk substrate is often believed to annihilate the generation of any measurable streaming potential even though $\zeta$-potential values are reported in literature for metallic surfaces [5,12-17]. Already in the 1930s, the famous Kruyt and Overbeek school of physics and chemistry of colloids at Utrecht University (The Netherlands) recognized the option of electron exchange between an electronically conducting substrate and an electrolytic aqueous medium, as well as the pertaining consequences for the traditional methodologies of measuring electrokinetic quantities [18-21]. Still, in those early days the fundamental aspects of the corresponding conduction *via* metallic substrates in terms of their impact on the apparent magnitudes of the electrokinetic parameters were not available. With the current insight into surface conduction effects on electrokinetic parameters [22-28] and a well-developed state of electrodic chemistry of bipolar faradaic reactions [29-31], it seems timely to get back to the subject and aim for a description of the basic processes in situations where electrode kinetics interfere with the generation of streaming potential by electron-conducting substrates. This article aims to outline these basic concepts as well as some practical utilities that emerged.

## 2. Faradaic depolarisation in the electrokinetics of some metal/electrolyte solution interfaces

### 2.1. Electrokinetics of metallic surfaces in inert electrolytes.

When referring to electrokinetics of (polarisable) metallic surfaces, one thinks about a number of non-linear electrokinetic phenomena that are now extensively detailed in literature, *e.g*. the superfast

electrophoresis of metallic particles [32], the self-assembly of colloids at electrode surfaces [33], the AC electroosmosis at electrode arrays [34], or induced charge electroosmotic processes and their applications in microfluidics [35]. This article focuses on the situation where deviations from the standard linear electrokinetic response stem from electron transfer reactions generated under lateral flow conditions in streaming potential set-up (**Figure 1**). The first evidence for occurrence of such faradaic processes in a thin-layer cell classically employed for streaming potential measurements was reported by Duval et al. [36] in their study of the bipolar electrodic behaviour of aluminum wafers in inert $KNO_3$ solution (**Figure 2**). In this work, a DC lateral potential with magnitude $\Delta\varphi_S$ is applied in the electrolyte chamber of the cell in order to mimic the development of streaming potential following applied flow. For sufficiently strong lateral DC fields, the Al is anodically dissolved at the negative side of the field in the bulk medium, whereas water is being reduced at the positive side (**Figures 2A,B**). Basically, this bipolar electrodic behaviour originates from the spatial distribution, along the metallic substrate, of the local potential drop between bulk solution and equipotential surface, denoted hereafter as $V(y)$ where *y* is the direction parallel to the duo of bipolar electrodes. When locally the anodic and cathodic overpotentials exceed values in line with electron transfer occurrence, then a bipolar current , denoted as $I_f$ , flows in the cell where *e-* are produced at the anodic end of the bipolar electrode and are consumed at the other cathodic side (**Figure 2B**). In steady state, the amount of charges supplied to the bipolar set of electrode areas is the same, except for the sign. In turn, the bipolar current $I_f$ corresponds to the spatial integration of the local anodic or cathodic faradaic current density along the substrate. As demonstrated in [36], there is a connection between the local potential $V(y)$-current density (denoted as $j(y)$) relationship operational at a given position *y* and the conventional monopolar current densities, measured *e.g.* by cyclic voltammetry (**Figure 2C**), that follow conventional Butler-Volmer electron transfer kinetics [37,38]. As a first order approach, assuming that the electric field remains constant in solution, the use of monopolar electrochemical data properly projected on the *y*-direction allows a straightforward derivation of the spatial distribution of the faradaic current density along the bipolar substrates and thus an estimation of the bipolar current after adequate integration over the spatial scale *y*. Such strategy allows for a quantitative interpretation of Al bipolar dissolution over time (**Figure 2A**) as well as the evaluation of the total current $I_f + I_\Omega$ flowing in the cell as a function of the applied field in solution, with $I_\Omega$ the ohmic contribution that depends on the electrolyte concentration **(Figure 2D)**. In **Figure 2**, the rates of electron transfer reactions are determined by the kinetics of electron exchange reactions at the conducting substrates: this is the case of irreversible electrodics. Accordingly, the potential drop across the cell required for anodic and cathodic electron transfers to occur concomitantly is rather large (about 3 V for the $Al/KNO_3$ electrolyte system, see **Figure 2C**) and this potential drop can never be reached under common lateral flow conditions that generate streaming potentials, denoted hereafter as $V_{str}$ , whose

magnitude (in absolute value) never exceed the order of 100 mV. These elements explain why the streaming potential of metals in standard indifferent electrolytes obeys the conventional Helmholtz-Smoluchowski equation [1] with no impact of bipolar electronic conduction and with a respected linearity between $V_{str}$ and applied pressure $\Delta P$. This linearity is well evidenced for streaming potentials measured on *e.g.* aluminum or gold at various values of solution pH (**Figure 3**). Altogether, the activation potential for bipolar faradaic processes is never reached for electrochemically irreversible systems under lateral flow conditions.

An extension of the Helmholtz-Smoluchowski (H-S in short) expression with account for bipolar electronic conduction process may be written in the simple form for the configuration given in **Figure 1** [15]

$$V_{str} = \frac{\varepsilon_0 \varepsilon_r \zeta \Delta P}{\eta\left(K^L + 2K^\sigma / a + 2K^f\right)} \quad (1)$$

, where $\varepsilon_0$ is the dielectric permittivity of vacuum, $\varepsilon_r$ the relative dielectric permittivity of the solution, $\eta$ the viscosity of the solution, $a$ the distance between the two flat surfaces (**Figure 1**), $K^L$ the specific bulk electrolyte conductivity ($\Omega^{-1}$ m$^{-1}$) and $K^\sigma$ the specific (ionic) surface conductivity ($\Omega^{-1}$). $\zeta$ is the electrokinetic potential of the metallic surfaces considered, and $K^f$ is the specific bipolar faradaic conductivity ($\Omega^{-1}$ m$^{-1}$) for one metallic substrate defined by $K^f = \left(I_f / V_{str}\right)C^{-1}$ with $C$ (m$^{-1}$) the cell constant given by $C = L_0 / \left(al\right)$ (see footnote [⊥]), $L_0$ and $l$ being the length and width of the metallic substrates mounted parallel in the streaming potential set-up, respectively (**Figure 1**). The case tackled in the current section where the rates of the bipolar faradaic reactions are significantly determined by electron transfer kinetics corresponds to Eq. (1) taken in the limit $K^f << K^L/2 + K^\sigma / a$, which reduces to the classical H-S equation from which $\zeta$-potential can be simply derived from the slope of the linear regression of measured $V_{str}$ as a function of applied pressure $\Delta P$ (**Figure 3**). We note that the Dukhin number $Du = K^\sigma / \left(aK^L\right)$ quantifying the importance of surface conductivity to the generation of streaming potential has the dimensionless equivalent $K^f / K^L$ that reflects the contribution by bipolar electronic conduction.

2.2. Electrokinetics of metallic surfaces depolarised by bipolar faradaic reactions.

Another type of electron transfer machinery is obtained by addition of a redox couple into the medium. Such a couple should be able to transport electrons to or from the metallic surface in agreement with the local Nernstian potential of the DC field in solution. Generally, a redox couple

[⊥] There is a mistake in Eq. (5) of reference [15] where $l$ should be replaced by $la / L_0$.

should be chosen with a sufficiently strong electrochemical reversibility such that depolarisation rates are not limited by slow electron transfer at the metal/medium interface. Under this condition, the local faradaic current along the bipolar substrate is significantly controlled by the mass transfer of the redox species to/from the conducting surface. The couple $Fe(CN)_6^{3-}/(Fe(CN)_6^{4-}$ on a gold surface is quite suitable in this respect, with the additional attractive feature that the diffusion coefficients of the two species are the same. Owing to the significant reversibility of the electron transfer reactions taking place between metallic substrate and $Fe(CN)_6^{3-}/(Fe(CN)_6^{4-}$ redox species [5,15], it is anticipated that bipolar electronic conduction should be operational already at low streaming potential values or, equivalently, at low applied pressure drops $\Delta P$ (**Figure 4A)**. The occurrence of such a bipolar electronic conduction sustained by the $Fe(CN)_6^{3-}/(Fe(CN)_6^{4-}$ couple at a gold surface is confirmed by streaming potential data $V_{str}$ *vs.* $\Delta P$ measured for flat gold layers at different solution pHs (**Figure 4B)** and at various bulk concentrations of redox species (denoted as $c_O^*$ and $c_R^*$ for the oxidized and reduced species, respectively) [15]. The results evidence that the electrokinetic response deviates from linearity at significantly large $V_{str}$ achieved for pH values that are sufficiently higher than the isoelectric point of the gold surface material whose double layer features result generally from the coupling between electronic and ionic charging mechanisms (so-called amphifunctional double layers, [39,40]). This condition ensures indeed that the magnitude of the bipolar current and, therewith, that of the bipolar conductance term in Eq. (1) becomes significant or even dominant over the bulk solution and surface conductance contributions. With increasing $c_O^*$ and $c_R^*$, the streaming potential response with applied pressure further increasingly deviates from the classical linear H-S behavior (see Figure 11 in [15]), which highlights not only the growing importance of the bipolar conduction term $K^f$ in Eq. (1) under such conditions, but also the existence of a non-linear dependence of $K^f$ on $\Delta P$. Quantitative elaboration of $K^f$ for reversible bipolar electrodic reactions calls for the corresponding computation of the bipolar faradaic current $I_f$ as a function of applied pressure $\Delta P$ and streaming potential $V_{str}$. Assuming full reversibility of electron transfer at every position *y* along the bipolar electrodes and a linear distribution for the overpotential *V* in this *y*-direction, an approximate expression can be derived for $K^f$ and, by extension, for Eq. (1). The result reads as (see footnote [×])

$$V_{str} = \frac{\varepsilon_0 \varepsilon_r \zeta \Delta P}{\eta\left( K^L + \frac{2K^\sigma}{a} + \frac{9}{10}\left(\frac{2L_0}{5}\right)^{5/3} \eta f \frac{\beta}{a} c_{redox}^* \left(\Delta P\right)^{1/3} \right)} \qquad (2)$$

, which is applicable to fully reversible bipolar electrodics with $c_{redox}^* = c_O^* = c_R^*$. In Eq. (2),

[×] Unlike Eq. (21) in reference [15], this equation integrates the correct definition of the specific bipolar faradaic conductivity. Note that this conductivity varies with hydrodynamic terms and redox terms.

$f = F/(RT)$ with *F*, *R* and *T* having their classical meanings and $\beta = 0.42nF\left[aD^2/(\eta L_o)\right]^{1/3}$ with $n$ the number of electrons involved in the anodic and cathodic faradaic reactions and *D* is the diffusion coefficient of O and R species taken identical for the sake of simplicity. As discussed in [15], the validity of the homogeneous field approach and hence of Eq. (2) depends on the magnitude of the ratio $I_f / I_\Omega$ and even at low field strengths in solution and low bulk concentrations of redox components, this approach may lead to inappropriate results, as will be further discussed in the next section. Nevertheless, Eq. (2) has the merit to provide a simple qualitative extension of the H-S equation that includes a bipolar conductance $K^f$ exhibiting a dependence on $(\Delta P)^{1/3}$, of which the origin is to be found in the non-linear profile of the diffusion layer thickness along the bipolar electrodes under lateral flow conditions [15,41]. The underlying power-law variation of $V_{str}$ with increasing $\Delta P$ qualitatively agrees with the data in **Figure 4B**. For an extensive discussion of the above results, the reader is referred to the original work [15].

2.3. Rigorous elaboration of the dependence of the bipolar faradaic current on lateral electric field and applied pressure.

In its most rigorous form, the evaluation of the bipolar faradaic current under lateral flow conditions is not an easy task as it involves non-linear couplings between electrostatics, hydrodynamics, electrode kinetics and redox concentration polarisation features that are spatially distributed along the bipolar electrodes (*y* dimension) and/or in the direction perpendicular to the metal/medium interfaces (*x* direction), as schematised in **Figure 5**. In detail, the transversal overpotential $V(y)$ driving the electron transfer at position *y* along the bipolar electrodes generally depends on *y* in a non-linear way, *i.e.* the lateral field in solution can not be *a priori* considered homogeneous. This non-linearity arises from the electroneutrality condition that holds in any electrolyte volume of infinitesimal length d*y* located between the two metallic substrates mounted parallel to each other in the cell and depolarised by bipolar faradaic reactions (**Figure 1**) [29]. This condition leads to a differential equation that couples $V(y)$ to the local faradaic current density $j(y)$ and the bulk electrolyte conductivity $K^L$ according to [29]

$$aK^L \mathrm{d}^2V(y)/\mathrm{d}y^2 + 2j(y) = 0 \qquad (3)$$

, with boundaries given by $V(y = -L_0/2) - V(y = +L_0/2) = V_{str}$ and $\mathrm{d}V/\mathrm{d}y\big|_{y=-L_0/2} = \mathrm{d}V/\mathrm{d}y\big|_{y=+L_0/2}$ [29,30]. The latter equation reflects the condition of no charge accumulation in the bipolar substrates and the positions $y = \pm L_0/2$ correspond to the ends of the bipolar electrodes (**Figure 5**). Eq. (3) is valid under practical streaming potential measurement conditions for the reasons set forth in [29-31], in particular the substrate/medium double layer

thickness is much smaller than the gap *a* and the thickness of the diffusion layer developed along the bipolar electrodes. It is inferred from Eq. (3) that the limit of homogeneous field in solution is reached only for insignificant bipolar current $I_f$ compared to the ohmic current $I_\Omega\left(=K^L V_{str} C^{-1}\right)$. An additional complexity stems from the two-dimensional spatial distribution of the concentrations of the active redox species due to the lateral pressure-driven convection and the transversal diffusion processes (**Figure 5**). The resulting polarisation of the redox species concentration in the thin-layer cell necessarily needs to be accounted for electron transfer reactions that exhibit some degree of reversibility. The concentration profile, *e.g.* for the O species, is then determined by the convective diffusion equation recast in the form [31]

$$v^0\left(1-X^2\right)\frac{\partial C_O(X,Y)}{\partial Y}=\frac{4D_O L_0}{a^2}\frac{\partial^2 C_O(X,Y)}{\partial X^2} \tag{4}$$

, where the quantities *x*, *y* and the local concentration $c_O(x,y)$ are here scaled according to $X=2(x-a/2)/a$, $Y=(y+L_0/2)/L_0$ and $C_O(X,Y)=\left(c_O(X,Y)-c_O^*\right)/c_O^*$, respectively, $v^0=a^2\Delta P/(8\eta L_0)$ is the bulk fluid velocity at the centre of the cell ($X=0$) and $D_O$ is the diffusion coefficient of the oxidized species. An equation analogous to Eq. (4) holds for the reduced species R [31]. The boundary conditions associated to Eq. (4) and operative at the medium/solution interfaces $(X=\pm 1)$ (**Figure 5**) translate the coupling between the mass balance for O and R chemicals at these positions and the rate of the interfacial electron-transfer reactions given by the Butler-Volmer expression, *i.e.* [31]

$$j(Y)=nFk_o\left\{-c_O(X=\pm 1,Y)\exp\left[nf\alpha\left(V(Y)-V^o\right)\right]+\right.$$
$$\left.c_R(X=\pm 1,Y)\exp\left[-nf(1-\alpha)\left(V(Y)-V^o\right)\right]\right\} \tag{5}$$

, where $j(Y)$ is coupled to the gradients of O and R concentrations at $X=\pm 1$ [30,31], $k_o$ is the standard (or intrinsic) rate constant for electron transfer reaction, and it can be corrected for electric double layer potential *via* proper Frumkin modifications of the exponential arguments in Eq. (5) [37]. $\alpha$ $(0\le\alpha\le 1)$ is the transfer coefficient and $V^o$ is minus the standard potential of the O/R redox couple. Once the distributions of the potential $V(y)$ and of the faradaic current density $j(Y)$ are obtained from the numerical solution of Eqs (3)-(5) along the lines detailed in [31], the bipolar current $I_f$ can be computed from integration of $j(Y)$ over the anodic or cathodic surface area of the bipolar electrodes (**Figure 5**). **Figure 6** provides representative results for the dependence of $I_f$ on practical values of $k_o$ at various applied pressures $\Delta P$ (**Figure 6A**) and different lateral potential drops $\Delta\varphi_s=V(y=-L_0/2)-V(y=+L_0/2)$ (**Figure 6B**). For the sake of demonstration, $\Delta P$ and $\Delta\varphi_s$ are

considered independent of each other in **Figure 6**, *i.e.* the electrokinetic coupling between lateral field and flow is ignored here. This coupling is explicitly considered in the next section when referring to the estimation of $\zeta$-potentials of metallic substrates depolarised by bipolar faradaic processes. In line with expectation, **Figure 6A** shows the gradual increase of $I_f$ with $k_o$ and it highlights the presence of a plateau value reached at sufficiently large $k_o$. In the regime of low $k_o$, $I_f$ is essentially independent of the mass transport of the electroactive species as the only sluggish kinetics of the electron transfer reactions determines the rate of the bipolar faradaic reactions: this is the irreversible electrodic limit considered in [29]. In this limit, $I_f$ is independent of $\Delta P$ and of the diffusion features of O and R to/from the conducting surfaces. In the other extreme where interfacial electron transfer is fast, which is achieved at sufficiently large $k_o$, the plateau reached by $I_f$ increases with $\Delta P$. The rate of the bipolar faradaic reactions is here solely determined by the convective diffusion of O and R to/from the surfaces: this is the fully reversible electrodic situation specifically tackled in [30]. For intermediate $k_o$ values, the bipolar current is governed both by electron transfer kinetics and by the mass transfer of the electroactive species: this is the quasi-reversible electrodic case [31]. At fixed $k_o$ and for significant reversibility of the electron transfer, the increase of $I_f$ with $\Delta P$ originates from the local decrease of the diffusion layer at every position *y* along the bipolar electrodes. Similarly to monopolar faradaic reactions for which the appearance of kinetic effects depends on the time window of the experiment, the degree of reversibility for a bipolar process is clearly a function of the pressure gradient applied across the cell (**Figure 6A**). In particular, the irreversible limit is satisfied over a broader range of $k_o$ values with increasing $\Delta P$ as, then, the extent of O/R concentrations polarisations in the *x*-direction (**Figure 5**) is reduced due to the facilitated transport of the redox species by convection. Accordingly, the electron transfer step at the interface increasingly determines the rate of the faradaic reactions. For a given non-zero value of $\Delta\varphi_S$ (**Figure 6B**), the irreversible and reversible electrodic regimes can be identified in a way similar to that adopted in **Figure 6A**, *i.e.* from comparison of results obtained for finite $k_o$ (solid lines) and in the absence of redox concentration polarisation (dotted lines). In particular, under the pressure condition adopted in **Figure 6B**, the bipolar current corresponding to a fully reversible functioning of the faradaic processes reaches the diffusive limiting regime for extreme values of $\Delta\varphi_S$ (larger than 10 V in the example of **Figure 6B**). At intermediate value of $k_o$ (quasi-reversible behaviour of the electrodes), $I_f$ increases with $\Delta\varphi_S$ because the magnitudes of the local overpotentials $V(Y)$ and of the ensuing rates of O/R mass transfer increase. In turn, with increasing $\Delta\varphi_S$ the range of rate constants associated to the irreversible bipolar faradaic limit is gradually shifted to lower values of $k_o$, a feature that is further expected from classical electrodic theory for monopolar faradaic processes [38].

Altogether, the overall picture resulting from the data given in **Figure 6** and from the non-linear coupling between convective diffusion transport of electroactive species and electric potential distribution under conditions of finite local faradaic currents, is that the reversibility of the electron transfer reaction inherently varies with position along the bipolar substrates, with the highest reversibility achieved downstream. This specificity of bipolar electrodics as compared to conventional monopolar electrochemical reaction rates leads generally to asymmetric profiles of the faradaic current density along the surface and, therefore, of the overpotential $V(y)$ [31]. For further details, the reader is referred to a series of papers where the complete mathematical treatments of irreversible [29], reversible [30] and quasi-reversible [31] bipolar faradaic processes are available together with some analytical expressions derived wherever possible for $V$ , $j$ and $I_{\mathrm{f}}$ .

2.4. Application for the evaluation of zeta (ζ)-potentials of metallic substrates depolarised by bipolar faradaic processes.

In streaming potential measurements, the potential difference $V_{\mathrm{str}}$ develops due to the convective displacement of the (net) amount of mobile ionic countercharges located in the electric double layer at the metallic substrate/medium interface. In the presence of bipolar faradaic depolarisation process, the steady state condition of zero net current flowing in the cell implies that the streaming current $I_{\mathrm{str}}$ is counterbalanced by the ohmic and bipolar faradaic currents, $I_{\Omega}$ and $I_{\mathrm{f}}$ , respectively, and by the surface conduction current $I^{\sigma}$ (if applicable), as shown in **Figure 4A**. Realizing that the streaming current $I_{\mathrm{str}}$ is related to the ζ-potential of the substrate *via* the classical Smoluchowski expression $I_{\mathrm{str}} = al\varepsilon_0\varepsilon_{\mathrm{r}}\zeta\Delta P/(\eta L_0)$ [1], the above condition can be written [5,30,31]

$$\frac{\varepsilon_0\varepsilon_{\mathrm{r}}\zeta\Delta P}{\eta} = -L_0 K^{\mathrm{L}} \left.\frac{\partial V(y,\Delta\varphi_{\mathrm{S}}=V_{\mathrm{str}},\Delta P)}{\partial y}\right|_{y=y_0} + \frac{L_0}{al} I_{\mathrm{f}}(\Delta\varphi_{\mathrm{S}}=V_{\mathrm{str}},\Delta P) \qquad (6)$$

, where $y_0$ is the position along the bipolar electrodes where the faradaic current density is zero (*i.e.* $j(y=y_0)=0$ , **Figure 5**) and we made explicit in Eq. (6) that both lateral potential distribution $V(y)$ and bipolar current $I_{\mathrm{f}}$ depend on applied pressure $\Delta P$ and on lateral field $\Delta\varphi_{\mathrm{S}} = V_{\mathrm{str}}$ along the lines discussed in the previous section (**Figures 5-6**). Eq. (6) can be exploited to compute the response streaming potential ($V_{\mathrm{str}}$) *versus* applied pressure of a metallic substrate characterized by a given ζ-potential and depolarised by bipolar faradaic reactions that are either irreversible, reversible or quasi-reversible depending on solution composition and nature of the electroactive species (see §2.3, **Figure 6**). The idea is then to (i) evaluate the bipolar faradaic current over a range of lateral fields $\Delta\varphi_{\mathrm{S}}$ and applied pressures $\Delta P$ by means of adequate numerical theory [29,30,31] chosen in relation with the nature of the electroactive redox components in solution, which defines in turn an envelope of

equation $I_f\left(\Delta\varphi_S,\Delta P\right)$, (ii) compute the surface of equation $\frac{al\varepsilon_0\varepsilon_r\zeta\Delta P}{L_0\eta}+alK^L\left.\frac{\partial V\left(y,\Delta\varphi_S=V_{str},\Delta P\right)}{\partial y}\right|_{y=y_0}$, and finally (iii) determine the intersection line $\Delta\varphi_S$ *vs.* $\Delta P$ between the envelope and planar surfaces derived in (i) and (ii), respectively. This intersection line then corresponds to the searched $V_{str}$ *vs.* $\Delta P$ characteristics of the metallic substrate. **Figure 7A** illustrates graphically the procedure and results are further given in **Figure 7B** for the example situation of fully reversible bipolar electrodics and different values of ζ-potential. As expected from the approximate Eq. (2), bipolar faradaic processes lead to the partial or complete suppression of streaming potential at given $\Delta P$ as compared to cases where they are not operational (these latter cases refer to the classical linear H-S equation, see long dotted lines in **Figure 7B**). In addition, bipolar depolarisation of the metallic surfaces generate a non-linearity in the dependence of the streaming potential on applied pressure, a feature that is also transparent in Eq. (2) derived from the oversimplified representation of homogeneous field in solution. Comparison between predictions from Eq. (2) and exact numerical results further highlight that the former leads to an overestimation of the bipolar current and an underestimation of the streaming potential (in absolute value) regardless of the magnitude of the applied pressure. **Figure 7C** further confirms the increasing suppression of streaming potential $V_{str}$ with increasing bulk concentrations of the (here reversible) redox couple in solution with the two extremes $I_f << I_\Omega$ and $I_f >> I_\Omega$ corresponding to the linear H-S equation (*i.e.* Eq. (1) with $K^f \equiv 0$) and to the complete extinction of the electrokinetic signal $\left(V_{str}\to 0\right)$ over the whole range of applied pressures, respectively. For the sake of completeness, **Figure 7D** provides $V_{str}$ *vs.* $\Delta P$ plots derived in the most generic situation of quasi-reversible bipolar electrodics for various values of the kinetic constant $k_o$. The faster is the kinetics of electron transfer (*i.e.* the larger is $k_o$), the more significant becomes the suppression of the streaming potential, in line with the associated growing magnitude of the bipolar current (**Figure 6**). Close inspection of **Figures 7B-D** reveal the existence of two pressure regimes in the dependence of $V_{str}$ on $\Delta P$. At sufficiently low pressures, the observable non-linearity between $V_{str}$ and $\Delta P$ is connected to the predominant limitation of the bipolar faradaic current by convective diffusion of the redox species (see approximate Eq. (2) for orientation purposes). At sufficiently large pressures where concentration polarisation for O and R species becomes significantly reduced and rates of electron transfer increasingly determined by the very kinetics of the electron transfer step (**Figure 6**), the streaming potential varies linearly with pressure, in agreement with experimental data (**Figure 4B**). It can be shown that the corresponding slope is formally given by the expression [5]

$$\frac{V_{str}}{\Delta P}=\frac{2\varepsilon_0\varepsilon_r\zeta}{\eta L_0 K^L\omega\coth\left(\omega L_0/2\right)} \tag{7}$$

, with $\omega$ the scalar defined by $\omega = F\sqrt{k_0\left(c_O^* + c_R^*\right)/\left(RTaK^L\right)}$. Eq. (7) holds in the linear part of the streaming-potential response measured at sufficiently large $\Delta P$ (see **Figure 4B**), for a number $n$ of exchanged electrons equal to 1 and for an electrodic electron transfer coefficient $\alpha$ of 1/2. Extension of Eq. (7) to any values of $n$ and $\alpha$ is available in [42]. Eq. (7) is particular useful for the evaluation of ζ-potential from measured streaming potential data as given in **Figure 4B**. The evaluation requires the accessible slope $V_{str}/\Delta P$ and knowledge of the kinetic constant $k_0$ obtainable from analysis of monopolar cyclic voltammetry data measured as a function of potential scan rate for solution compositions (in particular background electrolyte concentration and redox concentrations) matching those adopted in the electrokinetic measurements [5]. Illustrative results are given in **Figure 8** for gold in $KNO_3$ electrolyte at different pH values and for different combinations of $Fe(CN)_6^{3-}/Fe(CN)_6^{4-}$ concentrations. They show that the magnitude of ζ-potentials estimated on the basis of Eq. (7) well compares, on a qualitative level, with that derived from measurements in the absence of electroactive species. In contrast, one obtains unrealistically high ζ-potentials values if considering (incorrectly) that full reversibility of electron transfer reactions applies over the whole range of applied pressures. In addition, monopolar electrochemical data highlight a significant degree of irreversibility for the electron transfer between $Fe(CN)_6^{3-}$ and $Fe(CN)_6^{4-}$ under practical electrokinetic conditions where background electrolyte is not in very large excess over the electroactive species (see Figure 8 in [5]). Quantitatively, differences between ζ-potentials properly derived in the presence and absence of electroactive species can be interpreted on the basis of electric double layer models featuring the adsorption of the multivalent anionic oxidized and reduced species on the gold surface (**Figure 8**) [5].

### 3. Faradaic double layer depolarisation in electrokinetics: Onsager relations

As mentioned in the Introduction, any electrokinetic investigation of an electronically conducting substrate normally has been surrounded by suspicions concerning the short-circuiting impact on the measurement. More often than not, substrate conduction may lead to substantial or even practically complete annihilation of the envisaged electrokinetic quantity (**Figures 7B-D**). Our inclusion of faradaic processes in electrokinetic experiments so far shows that indeed the presence of conducting surfaces generally affects the outcome of electrokinetic measurements. In order to better understand the extent of impact by faradaic reactions on electrokinetic signals it is mandatory to consider the electrodic features of the measurement situation [5]. First of all, the transfer of electrons at the substrate/medium interface should be sufficiently fast such that depolarisation rates are fast compared to the rate of establishing steady state electrokinetic conditions. In electrodic electrochemistry jargon this would come to requiring a sufficiently strong electrochemical reversibility. Interestingly, in the setting of an electrokinetic measurement cell this reversibility is effectively position-dependent, which further complicates the theoretical reconstruction, as discussed in the preceding sections. It should also

be added that depolarisation can be realized not only by electron transfer reactions (for metals), but also by ion transfer processes (in hydrogels and, more generally, soft surface layers [7-11, 43]). The underlying Onsager relationships are laid out in [44] and highlight the common basis for suppression of streaming potential either by ionic or electronic conduction processes. Reference [44] further discusses possible limitations of double layer polarisation by faradaic processes due to the finite electronic conductivity operational in the bulk substrate, a matter that may be of particular importance in electrokinetics of some semi-conducting materials.

**4. Bipolar electrochemistry beyond the electrokinetics framework**

The fundamental processes governing the non-linear coupling between bipolar electrodic kinetics and electrokinetics are reviewed in this study within the context of streaming potential generation at metallic surfaces. The possibility to control electroosmotic flow pattern in metallic chambers *via* exploitation of the intricate connection between bipolar faradaic current features (modulated by playing with the nature of the redox species in solution) and lateral electric field distribution has been further theoretically explored in literature [45,46]. Duval et al. [42] also showed, both experimentally and theoretically, how the non-linearity of the streaming potential-applied pressure response of metallic surfaces depolarised by bipolar electrodic reactions could be used for monitoring the coverage of adsorbed passivating particles on electron conducting substrates. Such adsorption may indeed partly or entirely block the occurrence of bipolar electronic conduction, which in turn leads to deviations from classical linear Helmholtz-Smoluchowski theory to an extent that depends on the surface concentration of the particulate passivators. The situation of a coupling between a lateral electric field -whether it is externally applied or generated under lateral flow conditions- and bipolar faradaic processes is further recurrent in a number of electroanalytical applications that have been reported in the last 20 years. For the sake of illustration, Chow et al. [47] designed a wireless electrochemical bipolar electrode microarray coupled to an electrogenerated chemiluminescence sensing system, which allows fine monitoring of the faradaic current at the cathodic part of the bipolar electrodes. Warakulwit et al. [48] demonstrated that the concept of bipolar electrochemistry could be easily adapted to generate dissymmetric metal-modified carbon nanotubes in an aqueous bulk phase using a simple capillary electrophoresis setup. Ulrich et al. [49] further showed how bipolar electrochemistry-based methods were suitable to design functional molecular gradients along conducting surfaces, exploiting here the fact that adsorption or desorption of specific molecules could be triggered through bipolar faradaic reactions. Also, Loget et al. [50] reported on the possible propulsion of conductive micro-objects by bipolar electrochemistry, with the motion of the metallic object being controlled by self-regenerating metal deposition and dissolution reactions taking place at the rear and front poles of the object. The reader is further referred to Fosdick et al. [51] and to Loget al. [52] for comprehensive reviews on various applications of bipolar electrochemistry, *e.g.* for sensing and screening purpose, for

the generation of electrical connection between metallic particles [53], or for the wireless spatial manipulation (translation, rotation or levitation) of conducting objects [50, 54-56].

## 5. Conclusions

Hans Lyklema has insisted a lot on the importance of surface conduction processes for a proper interpretation of electrophoresis data, analysis of the low frequency domain in dielectric spectra of colloids, and also for solving what he called the 'electrokinetic incongruence', *i.e.* without account of surface conduction term, electrokinetic measurements performed on a given material type with different equipments may provide different values with some of them being physically unrealistic or varying in a bizarre way with electrolyte concentration [22-27,57,58]. Accordingly, Hans recommended combining surface titration data (his focus was on particle dispersions) and surface conduction data for a proper interpretation of electrokinetic measurements [4,57,58]. The analogy with the account for bipolar electronic conduction in electrokinetics of metals seems to be quite strong. Indeed, we could argue that a proper evaluation of electrokinetics of metals requires combination with independent monopolar electrochemical measurements from which the bipolar electrodic determinants of the electron transfer reaction rates can be derived under given electrokinetic measurement conditions, such as the strength of the DC field across the bulk liquid medium. Subsequently, it can be decided whether or not these faradaic reactions interfere with streaming potential generation and ensuing zeta-potential values, pending proper implementation of the bipolar conduction term in the classical Helmholtz-Smoluchowski equation. The Bikerman expression for ion surface conduction [59-60] and its extension to include ion transport behind the shear plane [6] then leave place (or add to, depending on the systems considered) to the bipolar electronic conduction term elaborated on the basis of the Butler-Volmer kinetic equation and convective diffusion expression of electroactive redox species. As emphasized in this short review, the occurrence of bipolar faradaic processes under lateral flow conditions leads to the generation of a non-linear streaming potential-pressure response of metallic substrates with characteristics that are inherently functions of the electrode kinetic determinants of the electron-exchange rates and of the possible limitations of the conducting substrate in sustaining bulk electron transfer [44]. While the focus has been given so far on steady-state conditions, a remaining challenge includes the quantitative establishment of the dynamics underlying the coupling between bipolar electrode kinetics and electrohydrodynamics of electronic conductors, a demanding effort that is all the more pressing as the dimension of fluidic channels in current nanofluidic applications is comparable to typical extensions of electric double layers under practical salt concentration conditions [61-64].

This review portrays the current insight into interfacial properties of conducting surfaces under various chemical and electrochemical conditions. The basic elements delineated here are not only relevant for achieving a comprehensive picture of the coupling between electrode kinetics and bipolar electrodics. They also pave the way for possible wireless electrochemically-based control of electric

fields patterning in micro- and nano-fluidic chambers, with potential applications *e.g.* in the manipulation of particles or biological cells [65-67], and for the spatially-resolved detection of electroactive analytes in sensor devices whose functioning calls for bipolar electrochemistry principles.

**Declaration of competing interest**

None.

**References**

[1] Lyklema J. In Fundamentals of Interface and Colloid Science, Volume II: Solid-liquid interfaces; Chapter 4 *Electrokinetics and Related Phenomena*, Academic Press, London, 1995.

[2] Lyklema J. In Fundamentals of Interface and Colloid Science, Volume II: Solid-liquid interfaces; Chapter 3 *Electric Double Layers*, Academic Press, London, 1995.

[3] Lyklema J, Overbeek J Th G. On the interpretation of electrokinetic potentials. J. Colloid Sci 1961;16:501-512

[4] Lyklema J. Interfacial Potentials: Measuring the Immeasurable? Substantia 2017;1(2):75-93.

[5] Duval JFL. Electrokinetics of the amphifunctional metal/electrolyte solution interface in the presence of a redox couple. J Colloid Interface Sci 2004;269:211-223.

[6] Delgado A.V., Gonzales-Cabalerro F, Hunter RJ, Koopal LK, Lyklema J. Measurement and interpretation of electrokinetic phenomena. Pure Appl Chem 2005;77,1753-1805.

[7] Ohshima H. Electrophoresis of soft particles. Adv Colloid Interface Sci 1995;62:189-235.

[8] Duval JFL, Gaboriaud F. Progress in electrohydrodynamics of soft microbial particle interphases. Curr Opin Colloid Interface Sci 2010;15:184-195.

[9] Zimmermann R, Dukhin SS, Werner C, Duval JFL. On the use of electrokinetics for unraveling charging and structure of soft planar polymer films. Curr Opin Colloid Interface Sci 2013;18:83-92.

[10] Zimmermann R, Werner C, Duval JFL. Recent progress and perspectives in the electrokinetic characterization of polyelectrolyte films. Polymers 2016;8:7-23.

[11] Duval JFL, Werner C, Zimmermann R. Electrokinetics of soft polymeric interphases with layered distribution of anionic and cationic charges. Curr Opin Colloid Interface Sci 2016;24:1-12.

[12] Boulangé-Petermann L, Doren A, Baroux B, Bellon-Fontaine M-N. Zeta potential measurements on passive metals. J Colloid Interface Sci 1995;171:179-186.

[13] Berg JM, Romoser A, Banerjee N, Zebda R, Sayes C. The relationship between pH and zeta potential of ~30 nm metal oxide nanoparticle suspensions relevant to in vitro toxicological evaluations. Nanotoxicology 2009;3:276-283.

[14] Mikolajczyk A, Gajewicz A, Rasulev B, Schaeublin N, Maurer-Gardner E, Hussain S, Leszczynski J, Puzyn T. Zeta potential for metal oxide nanoparticles: a predictive model developed by a nano-quantitative structure-property relationship approach. Chem Mater 2015;27:2400-2407.

[15] Duval JFL, Huijs GK, Threels WF, Lyklema J, van Leeuwen HP. Faradaic depolarization in the electrokinetics of the metal-electrolyte solution interface. J Colloid Interface Sci 2003;260:95-106.

[16] Bellmann C, Opfermann A, Jacobasch H-J, Adler H-J. Characterisation of pure or coated metal surfaces with streaming potential measurements. Fresenius J Anal Chem 1997;58,255-258.

[17] Exartier C, Maximovitch S, Baroux B. Streaming potential measurements on stainless steels surfaces: evidence of a gel-like layer at the steel/electrolyte interface. Corrosion Sci 2004;46:1777-1800.

[18] Oosterman J. PhD thesis, University of Utrecht, The Netherlands, 1937.

[19] Kruyt HR, Oosterman J. Elektrokinese an metallen. Kolloid-Beih 1938;48,377-430.

[20] Overbeek J Th G. PhD Thesis *Theory of Electrophoresis, the Relaxation Effect*, University of Utrecht, The Netherlands, 1941.

[21] Overbeek J Th G. Theorie der Elektrophorese. Kolloid-Beih 1943;54,287-364.

[22] Lyklema J. Joint development of insight into colloid stability and surface conduction. Colloids Surf, A Physicochem Eng Asp 2014;440:161-169.

[23] Lyklema J, Minor M. On surface conduction and its role in electrokinetics. Colloids Surf, A Physicochem Eng Asp 1998;140:33-41.

[24] Lyklema J. Surface conduction. J Phys Condens Matter 2001;13:5027-5034.

[25] Kijlstra J, van Leeuwen HP, Lyklema J. Effects of surface conduction on the electrokinetic properties of colloids**.** J Chem Soc Faraday Trans 1992;88:3441-3449.

[26] Dukhin SS, Derjaguin BV. In Electrokinetic Phenomena, John Wiley and Sons, New York, 1974

[27] Dukhin SS, Zimmermann R, Werner C. Surface conductivity reveals counterion condensation within grafted polyelectrolyte layers. J Phys Chem B 2007;111:979-981

[28] Das S, Chakraborty S. Effect of conductivity variations within the electric double layer on the streaming potential estimation in narrow fluidic confinements. Langmuir 2010;26:11589-11596.

[29] Duval JFL, Minor M, Cecilia J, van Leeuwen HP. Coupling of lateral electric field and transversal faradaic processes at the conductor/electrolyte solution interface. J Phys Chem B 2003;107:4143-4155.

[30] Duval JFL, van Leeuwen HP, Cecilia J, Galceran J. Rigorous analysis of reversible faradaic depolarization processes in the electrokinetics of the metal/electrolyte solution interface. J Phys Chem B 2003;107:6782-6800.

[31] Duval JFL, Buffle J, van Leeuwen HP. Quasi-reversible faradaic depolarisation in the electrokinetics of the metal/solution interface. J Phys Chem B 2006;110:6081-6094.

[32] Dukhin SS. Electrokinetic phenomena of the second kind and their applications. Adv Colloid Interface Sci 1991;35:173-196.

[33] Prieve DC, Sides PJ, Wirth CL. 2-D assembly of colloidal particles on a planar electrode. Curr Opin Colloid Interface Sci 2010;15:160-174.

[34] Ramos A, Morgan H, Green N G, Castellanos A. AC Electric-field-induced fluid flow in microelectrodes. J Colloid Interface Sci 1999;217:420-422.

[35] Bazant MZ, Squires TM. Induced-charge electrokinetic phenomena: theory and microfluidic applications. Phys Rev Lett 2004;92:066101.

[36] Duval J, Kleijn JM, van Leeuwen HP. Bipolar electrode behaviour of the aluminium surface in a lateral electric field. J Electroanal Chem 2001;505:1-11.

[37] Conway BE. In *Theory and Principles of Electrode Processes*, Ronald Pr., New-York, 1965, Chapters 4, 5 and 6.

[38] Bard AJ, Faulkner LR in *Electrochemical Methods Fundamentals and Applications*, Eds. John Wiley and Sons, 2001, Second Edition, Chapter 3.

[39] Duval J, Lyklema J, Kleijn JM, van Leeuwen, HP. Amphifunctionally electrified interfaces: coupling of electronic and ionic surface-charging processes. Langmuir 2001;17: 7573-7581.

[40] Duval J, Kleijn JM, Lyklema J, van Leeuwen, HP. Double layers at amphifunctionally electrified interfaces in the presence of electrolytes containing specifically adsorbing ions. J. Electroanal. Chem 2002; 532:337-352.

[41] Levich VG in *Physicochemical Hydrodynamics*, Prentice-Hall, Englewood Cliffs, NJ, 1962.

[42] Duval JFL, Sorrenti E, Waldvogel Y, Gorner T, De Donato P. On the use of electrokinetic phenomena of the second kind for probing electrode kinetic properties of modified electron-conducting surfaces. Phys Chem Chem Phys 2007; 9:1713-1729.

[43] Zimmermann R, Gunkel-Grabole G, Bunsow J, Werner C, Huck WTS, Duval JFL. Evidence of ion-pairing in cationic brushes from evaluation of brush charging and structure by electrokinetic and surface conductivity analysis. J Phys Chem C 2017;121:2915-2922.

[44] Van Leeuwen HP, Duval, JFL. Faradaic double layer depolarization in electrokinetics: Onsager relations and substrate limitations. J Colloid Interface Sci 2007;309:350-359.

[45] Qian S, Duval JFL. Modulation of electroosmotic flows in electron-conducting microchannels by coupled quasi-reversible faradaic and adsorption-mediated depolarization. J Colloid Interface Sci 2006;300:413-428.

[46] Qian S, Duval JFL. Coupling between electroosmotically driven flow and bipolar faradaic depolarization processes in electron-conducting microchannels. J Colloid Interface Sci 2006;297:341-352.

[47] Chow K-F, Mavré F, Crooks JA, Chang B-Y, Crooks RM. A large-scale, wireless electrochemical bipolar electrode microarray. J Anal Chem Soc 2009;131,8364-8365.

[48] Warakulwit C, Nguyen T, Majimel J, Delville M-H, Lapeyre V, Garrigue P, Ravaine V, Limtrakul J, Kuhn A. Dissymmetric carbon nanotubes by bipolar electrochemistry. Nano Lett 2008;8:500-504.

[49] Ulrich C, Andersson O, Nyholm L, Bjorefors F. Formation of molecular gradients on bipolar electrodes. Angew Chem Int Ed 2008;47:3034-3036.
[50] Loget G, Kuhn A. Propulsion of microobjects by dynamic bipolar self-regeneration. J Anal Chem Soc 2010;132:15918-15919.
[51] Fosdick SE, Knust KN; Scida K; Crooks RM. Bipolar Electrochemistry. Angew Chem Int Ed 2013;52:10438-10456.
[52] Loget G, Zigah D, Bouffier L, Sojic N, Kuhn A. Bipolar electrochemistry: from materials science to motion and beyond. Acc Chem Res 2013;46:2513-2523.
[53] Bradley J-C, Chen HM, Crawford J, Eckert J, Ernazarova K, Kurzeja T, Lin MD, McGee M, Nadler W, Stephens SG. Creating electrical contacts between metal particles using directed electrochemical growth. Nature 1997;389:268-271.
[54] Loget G, Larcade G, Lapeyre V, Garrigue P, Warakulwit C, Limtrakul J, Delville M-H; Ravaine V, Kuhn A. Single point electrodeposition of nickel for the dissymmetric decoration of carbon tubes. Electrochim Acta 2010;55:8116-8120.
[55] Fattah Z, Loget, G, Lapeyre,V, Garrigue P, Warakulwit C, Limtrakul J, Bouffier L, Kuhn A. Straightforward single-step generation of microswimmers by bipolar electro-chemistry. Electrochim Acta 2011;56:10562-10566.
[56] Loget G, Kuhn A. Bipolar electrochemistry for cargo-lifting in fluid channels. Lab Chip 2012;12: 1967-1971.
[57] Lyklema J. On the slip process in electrokinetics. Colloids Surf, A Physicochem Eng Asp 1994;92:41-49.
[58] Lyklema J. Molecular interpretation of electrokinetic potentials. Curr Opin Colloid Interface Sci 2010;15:125-130.
[59] Bikerman JJ. Ionic theory of electroosmosis, streaming current and surface conductivity. Z Phys Chem A 1933;163:378-394.
[60] Bikerman JJ. Die Oberflächenleitfähigkeit und ihre Bedeutung. Kolloid Z. 1935;72:100-108.
[61] Daiguji H, Yang PD, Majumdar A. Ion transport in nanofluidic channels. Nano Lett 2004;4:137-142.
[62] Cervera J, Schiedt B, Neumann R, Mafe S, Ramirez P. Ionic conduction, rectification, and selectivity in single conical nanopores. Ionic conduction, rectification, and selectivity in single conical nanopores. J Chem Phys 2006;124:104706.
[63] Karnik R, Fan R, Yue M, Li D, Yang P, Majumdar A. Electrostatic control of ions and molecules in nanofluidic transistors. Nano Lett 2005;5:943-948.
[64] Pardon G, van der Wijngaart W. Modeling and simulation of electrostatically gated nanochannels. Adv Colloid Interface Sci 2013;199-200:78-94.
[65] Tenje M, Fornell A, Ohlin M, Nilsson J. Particle manipulation methods in droplet microfluidics. Anal Chem 2018;90:1434-1443.

[66] Luo T, Fan L, Zhu R, Sun D. Microfluidic single-cell manipulation and analysis: methods and applications. Micromachines 2019;10:104-134.

[67] Velve-Casquillas G, Le Berre M, Piel M, Tran PT. Microfuildic tools for cell biological research. Nano Today 2010;5:28-47.

## Figure captions

**Figure 1.** Typical configuration of a streaming potential set-up and characteristic dimensions of macroscopic surfaces adopted for experiments. In standard streaming potential set-ups, the cell gap $a$ may vary from several tens of microns up to the mm scale. $\Delta P$ is the applied pressure drop between the two reservoirs. The $x$, $y$ and $z$ directions are indicated. Reproduced from [36].

**Figure 2. (A)** Bipolar electrodic behavior of an aluminum surface placed in a thin-layer cell of the type given in Figure 1. Progression of the corroding edge with time (indicated) at a lateral potential $\Delta\varphi_S = 9$ V applied across the electrolyte chamber containing (here one) Al wafer, see scheme in Figure 1. Cell gap $a$ = 2.3 mm, $10^{-1}$ M $KNO_3$ concentration. **(B)** Schematics of the bipolar faradaic processes taking place in the thin-layer cell for an aluminum substrate in $KNO_3$ electrolyte. $I_f$ and $I_\Omega$ are the bipolar current and ohmic current in solution, respectively. **(C)** Voltammogram for monopolar Al substrate in $10^{-2}$ $KNO_3$ (scan rate: 30 $mVs^{-1}$). Potentials are given with respect to Ag/AgCl/KCl(sat) reference electrode. **(D)** Total current $I_f + I_\Omega$ flowing in the thin-layer cell of Figure 1 and measured for aluminum (symbols with solid lines as guides to the eye) and silica substrates (dotted lines, $I_f = 0$ by definition) at different $KNO_3$ electrolyte concentrations $10^{-1}$ M (a, a'), $5\times10^{-2}$ M (b, b'), $10^{-2}$ M (c, c'), $2\times10^{-4}$ M (d, d'). Scan rate (increasing potential $\Delta\varphi_S$): 30 mV $s^{-1}$. Cell gap $a$ = 0.2 mm. Panels (C) and (D) are reproduced from [36].

**Figure 3**. **(A)** Streaming potentials (symbols) measured on aluminum, gold and glass wafers (indicated) placed in the thin-layer cell depicted in Figure 1 (cell gap $a$ = 0.2 mm) using $10^{-3}$ M $KNO_3$ at different pH (indicated). **(B)** Streaming potentials (symbols) measured for gold at $10^{-3}$ M $KNO_3$ and various pH (indicated). Solid lines are linear regressions of the experimental data. Reprinted from J Colloid Interface Sci, Vol. 260, Duval JFL, Huijs GK, Threels WF, Lyklema J, van Leeuwen HP. Faradaic depolarization in the electrokinetics of the metal-electrolyte solution interface, 95-106. Copyright 2003 Elsevier.

**Figure 4**. **(A)** Schematic representation of the situation encountered in a streaming potential experiments performed in the presence of an electroactive redox couple $Fe(CN)_6^{3-}$ / $Fe(CN)_6^{4-}$. Under steady state conditions, the streaming current $I_{str}$ is counterbalanced by the ohmic current $I_\Omega$, the surface current $I^\sigma$ and the bipolar current $I_f$. **(B)** Streaming potentials measured for gold at different pH (indicated) in $10^{-3}$ M $KNO_3$ and $10^{-3}$M/$10^{-3}$M $Fe(CN)_6^{3-}$ / $Fe(CN)_6^{4-}$ concentrations (symbols). The solid curves are only guides for the eye and the dotted red lines are linear regressions of the data at sufficiently large applied pressure $\Delta P$ (see §2.4). Reprinted from J Colloid Interface Sci, Vol. 260, Duval JFL, Huijs GK, Threels WF, Lyklema J, van Leeuwen HP. Faradaic depolarization in the electrokinetics of the metal-electrolyte solution interface, 95-106. Copyright 2003 Elsevier.

**Figure 5.** Schematic representation of the bipolar faradaic depolarization process occurring in an electrokinetic cell under flow conditions. Convective diffusion of the redox components O (oxidized species) and R (reduced species) to/from the metallic surfaces takes place, which in turn generates a spatial distribution of the local current $j(y)$ along the electrodes. Integration of $j(y)$ over the relevant spatial areas (indicated) provides the bipolar current $I_f$. Depending on systems, the rate of electron transfer at the very electrode/solution interfaces ($x = 0$ and $x = a$) is governed by the mass

transport of the redox components to/from the solution (reversible electrodics), by the electron-exchange kinetic step (irreversible electrodics) or by both (quasi-reversible electrodics). The extent of reversibility of electron transfer is a further function of the lateral position *y* because the concentration polarization of O/R species and the overpotential $V(y)$ at the electrode/solution interface both vary along the bipolar substrate. $V^*$ corresponds to the value of the overpotential $V$ taken at the position $y = y_o$ where the current density is zero. The overall potential drop along the substrate is termed $V_{str}$ or $\Delta\varphi_S$ depending on whether or not coupling between lateral electric field in solution and applied pressure is considered. Generally, $y_o$ is not located at the middle of the surface due to asymmetry of the anodic and cathodic processes. See text for details. Reprinted from J Colloid Interface Sci, Vol. 260, Duval JFL, Huijs GK, Threels WF, Lyklema J, van Leeuwen HP. Faradaic depolarization in the electrokinetics of the metal-electrolyte solution interface, 95-106. Copyright 2003 Elsevier.

**Figure 6.** Typical theoretical dependence (symbols, and solid lines as guides to the eye) of the bipolar current $I_f$ on the kinetic rate constant $k_o$ at different applied pressure drops $\Delta P$ (indicated) across the thin-layer cell used for streaming-potential measurements **(A)**, and at different magnitudes of the lateral potential drop $\Delta\varphi_S$ (**B**). The dotted lines represent the bipolar current computed for irreversible anodic and cathodic reactions as specifically examined in [29]. Model parameters: $a$ = 0.2 mm, $L_0$ = 7.6 cm, $l$ = 2.6 cm, $D = 10^{-9}$ m$^2$ s$^{-1}$, $V^0$ = -233 mV, $K^L = 1\ \Omega^{-1}m^{-1}$, $\alpha = 0.5$, $c_O^* = c_R^* =$ 0.1 mM, $\Delta\varphi_S$ = 0.3 V **(A)** and $\Delta P = 1$ kPa **(B)**. Reproduced with permission from Duval JFL, Buffle J, van Leeuwen HP. Quasi-reversible faradaic depolarisation in the electrokinetics of the metal/solution interface. J Phys Chem B 2006;110:6081-6094. Copyright 2006 American Chemical Society.

**Figure 7. (A)** Graphical representation of the computational procedure for reconstruction of the streaming potential ($V_{str}$)-applied pressure ($\Delta P$) plots in the presence of here fully reversible bipolar faradaic processes ($k_o \to \infty$) generated under lateral flow conditions. The example is given for $\zeta$ = 100 mV, see text for details. **(B)**. Dependence of $V_{str}$ on $\Delta P$ for $\zeta = 150$ mV (a), 100 mV (b), 50 mV (c) and 8 mV (d). Symbols and short-dotted lines as guide lines to the eye: computations for bipolar reversible electron transfer reactions. The corresponding predictions based on standard Helmholtz-Smoluchowski equation (no bipolar surface conduction term is accounted for) and on the assumption of linear potential distribution in solution are displayed as long-dotted and solid lines, respectively. Model parameters in **(A)** and **(B)**: $a$ = 1 mm, $L_0$ = 7.6 cm, $l$ = 2.6 cm, $D = 5\times10^{-10}$ m$^2$ s$^{-1}$, $V^0$ = -233 mV, $K^L = 0.1\ \Omega^{-1}m^{-1}$, $\alpha = 0.5$, $c_O^* = c_R^* = 10^{-5}$ M. **(C)** Reconstruction of the streaming potential ($V_{str}$)-applied pressure ($\Delta P$) for different redox concentration $c^* = c_O^* = c_R^*$ (indicated) under fully reversible electron transfer conditions with $\zeta = 150$ mV. Other parameters: as in **(A)** and **(B)**. **(D)** Reconstruction of the streaming potential $V_{str}$-pressure $\Delta P$ plots with quasi-reversible bipolar electrodics theory for $\zeta = 100$ mV, and various electron-transfer rate constants: $k_o \to 0$ (a), $10^{-6}$ (b), $10^{-5}$ (c), $5\times10^{-5}$ m s$^{-1}$ (d), and $k_o \to \infty$ m s$^{-1}$ (e) (symbols and solid lines as guides to the eye). Other parameters: as in **(A)** and **(B)**. Data corresponding to situation (a) coincides with that calculated on the basis of the standard Helmholtz-Smoluchowski equation whereas the (solid) curve (e) pertains to the fully reversible bipolar faradaic depolarization of the double layer. The dotted lines are computed with neglect of concentration polarization. Panels **(A)** and **(B)** are reproduced with permission from Duval JFL, van Leeuwen HP, Cecilia J, Galceran J. Rigorous analysis of reversible faradaic depolarization processes in the electrokinetics of the metal/electrolyte solution interface. J Phys Chem B 2003;107:6782-6800. Copyright 2003 American Chemical Society. Panel **(C)** is reproduced from [5]. Panel **(D)** is reproduced with permission from Duval JFL, Buffle J, van Leeuwen HP. Quasi-reversible faradaic depolarisation in the electrokinetics of the metal/solution interface. J Phys Chem B 2006;110:6081-6094. Copyright 2006 American Chemical Society.

**Figure 8.** $\zeta$ -potentials calculated on the basis of Eq. (7) from streaming potential measurements performed on gold|($KNO_3$// $Fe(CN)_6^{3-}$ / $Fe(CN)_6^{4-}$) electrolyte interface as a function of solution pH (points). The long dotted line refers to $\zeta$ -potentials obtained for gold in the absence of redox species (absence of bipolar faradaic depolarization). The other lines refer to zeta-potential computations with the electric double layer model detailed in [5]. The bulk concentrations of the background $KNO_3$ electrolyte and of the redox species are indicated. Reproduced from [5].

## Figures

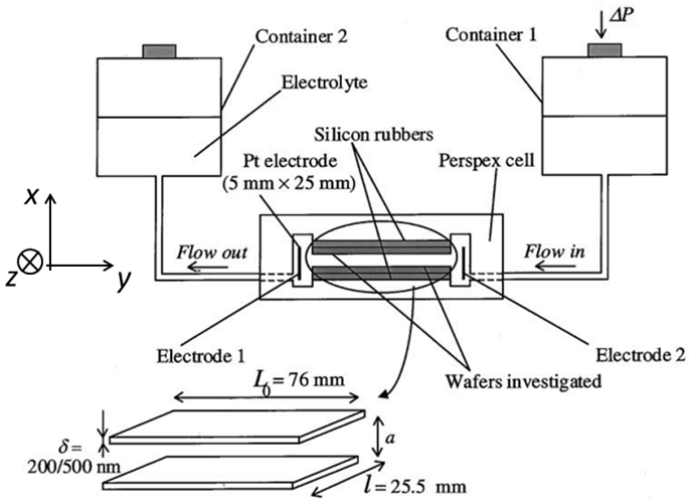


**Figure 1.**

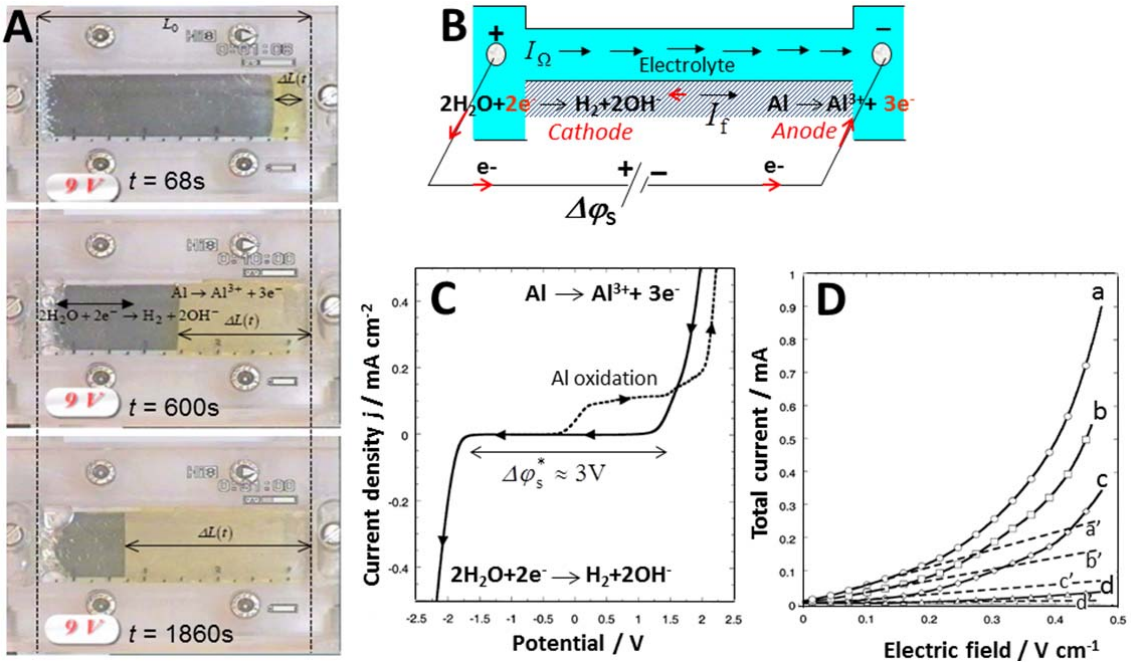


**Figure 2.**

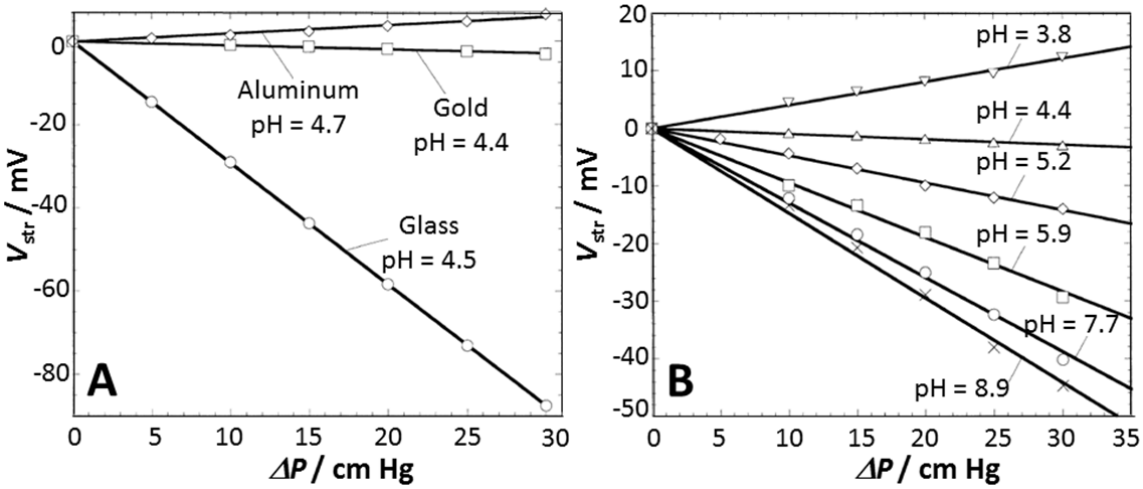


**Figure 3**.

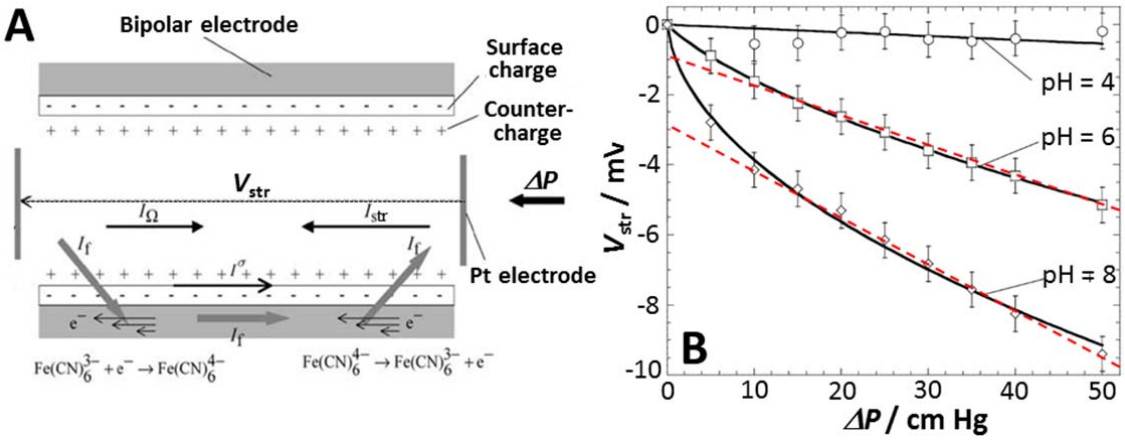


**Figure 4**.

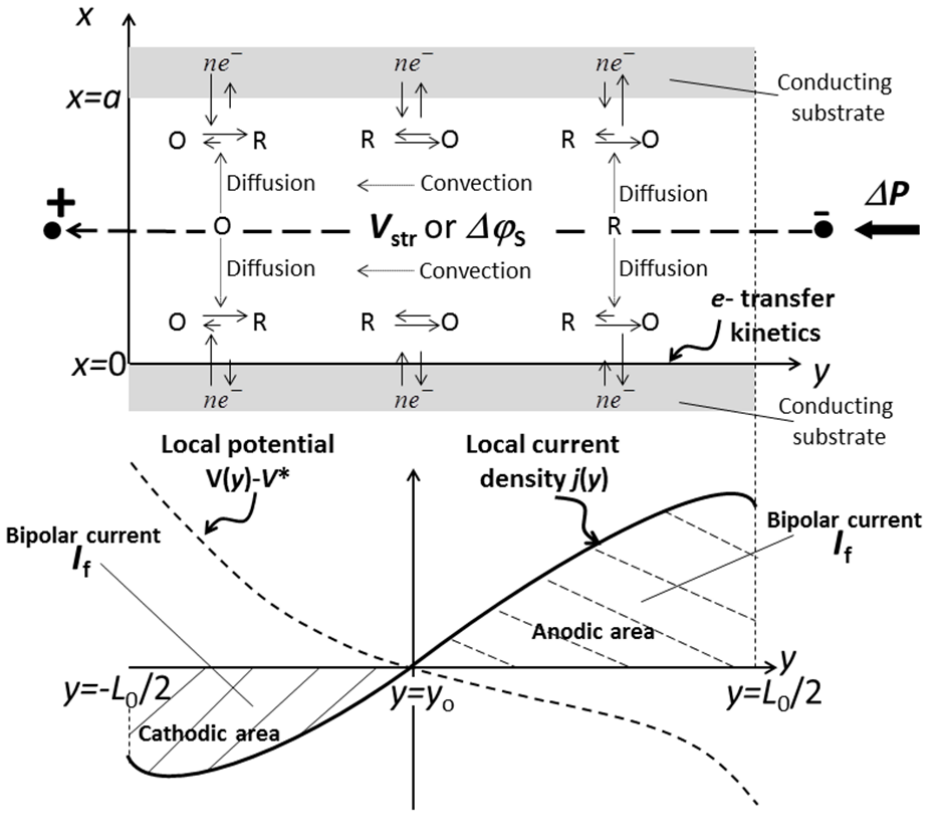


**Figure 5.**

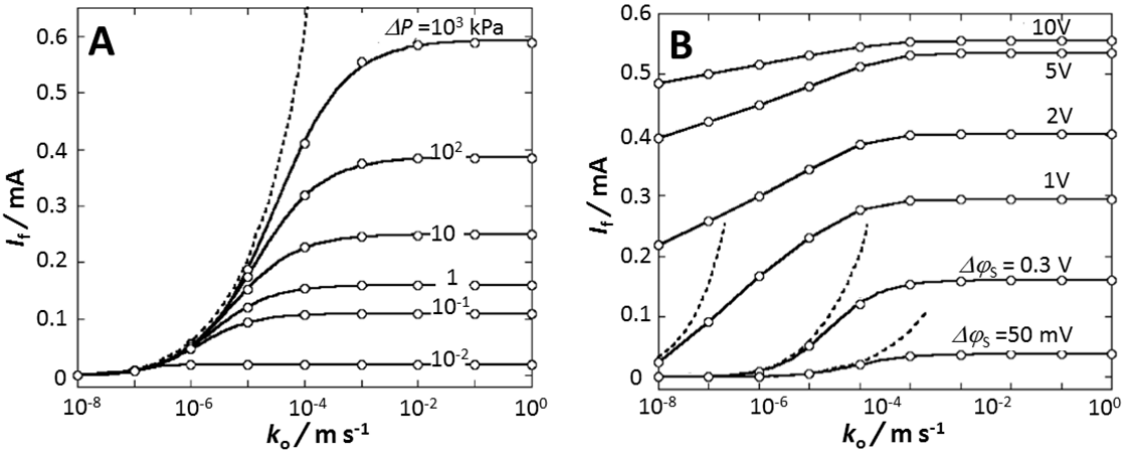


**Figure 6.**

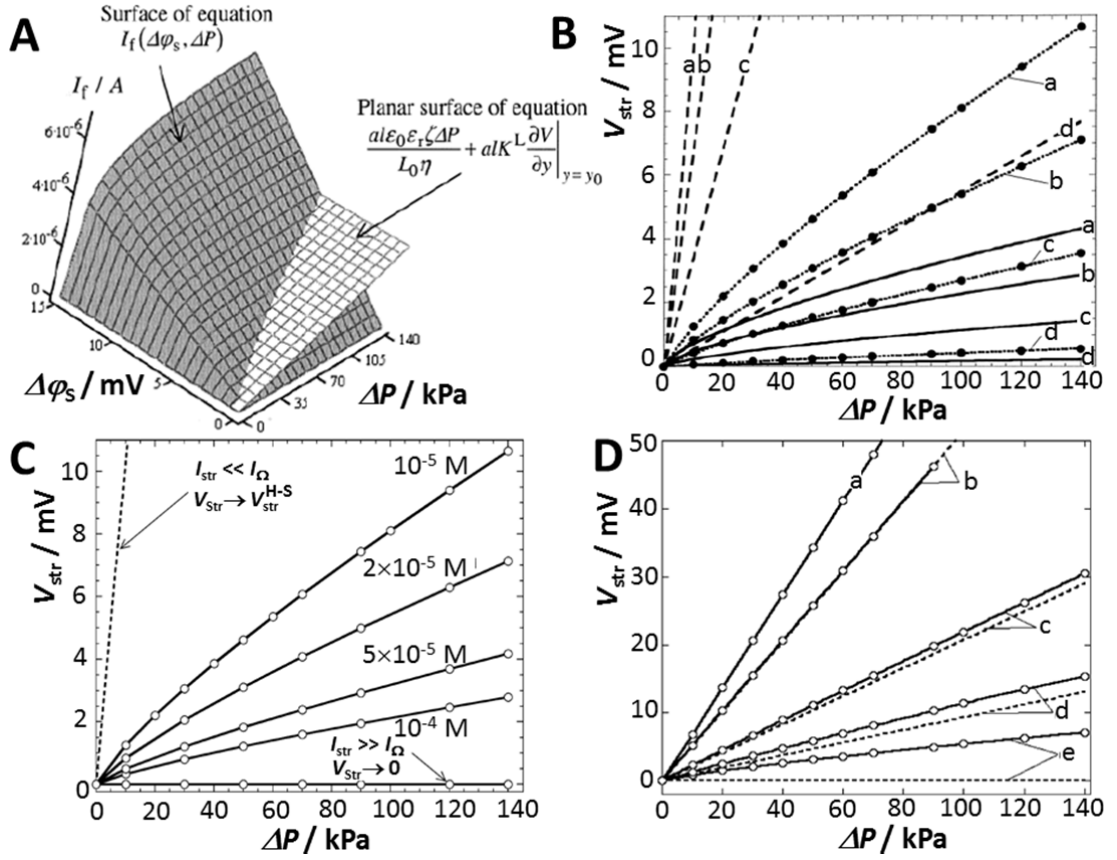


**Figure 7.**

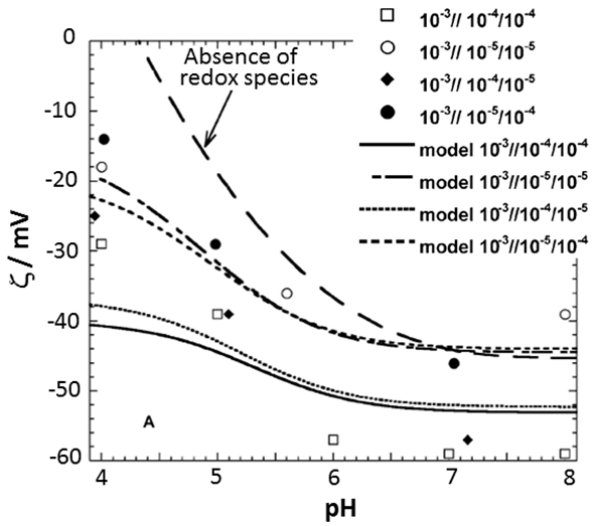
Absence of
redox species
10-3// 10-4/10-4
10-3// 10-5/10-5
10-3// 10-4/10-5
10-3// 10-5/10-4
model 10-3//10-4/10-4
model 10-3//10-5/10-5
model 10-3//10-4/10-5
model 10-3//10-5/10-4
ζ / mV
pH
A
0
-10
-20
-30
-40
-50
-60
4
5
6
7
8

**Figure 8.**